

Czesław NIŻANKOWSKI¹

HIGH PERFORMANCE OF NANOWIN™ GRINDING WHEELS

NanoWin™ grinding wheels represent the most recent generation of bound abrasive tools. They are characterized by the fact that the nanocrystalline sintered corundum immersed in the matrix of special ceramic glasscrystalline binder has been applied as abradant in them. In this paper, the results of comparative experimental tests of the cutting capacity of classical alundum, submicrocrystalline sintered corundum and NanoWin™ grinding wheels have been presented. The cutting capacities of the tested grinding wheels were determined with the application of the first McKee-Moor indicator. It was found that the cutting capacity of the tested grinding wheels in the process of hardened steel surface grinding stayed in the proportion of ca. 1 : 3 : 5, respectively.

1. INTRODUCTION

An extremely fast technical progress noted in recent years (according to Japanese sources, 6,000 new pieces of technical information are published every day) and a regular increase of customers' requirements cause the necessity of continuous improvement of product structures and means of production. New grades of hard-to-machine metal alloys, new types of ceramic-metal and metal-polymer composites, increased hardness of machined surfaces, new hot machining techniques and new grades of protective ceramic coating are supposed to ensure meeting of rigorous structural requirements, durability and reliability properties by products. At the same time, it is expected that the products will be produced effectively, which means that, with the application of the required quality and cost levels, productivity will be high. That situation enforces the application of modern production systems, together with modern machining tools. It also involves the application of bound grinding tools, including primarily grinding wheels. The classical grinding wheels made of noble alundum used up till now, made of ceramic feldspar binder, are characterized by low cutting capacity and low durability of the active grinding wheel surface (AGWS). For that reason, grinding wheels made of submicrocrystalline sintered corundum (Cubitron, VK, SG, Saphir Blue etc.) are widely applied concurrently for more than a decade. They contain modern, low-melting, ceramic binders of the types VH, VS, VBEM or VM. A great property of such grinding wheels is the abradant's self-sharpening capacity which

¹ Ośrodek Badawczo-Rozwojowy Sprzętu Mechanicznego w Tarnowie Sp. z o.o.

considerably extends the grinding wheel's durability and improves the machined surface's geometric structure quality. The abrasive grains of submicrocrystalline sintered corundum are in fact made of sintered Al_2O_3 crystallites, with the dimension ranging from 0.1 to 0.7 μm , and, during grinding, those grains are chipped off from the main grains, revealing new micro-blades located a layer below. A similar self-sharpening mechanism occurs during grinding with the wheels made of nanocrystalline sintered corundum grains, however, single crystallites from 10 to 40 nm are chipped off. That results from the fact that nanocrystalline sintered corundum grains are actually sintered from the crystallites which are by only one, not two, size orders smaller than those of the known submicrocrystalline sintered corundum. For that reason, the name of the binder is fairly conventional, although the difference in the properties in comparison to the submicrocrystalline sintered corundum is definitely essential. The grinding grains of the nanocrystalline sintered corundum are actually harder, more resistant to compression, more ductile and more resistant to abrasion due to their compact microstructure.

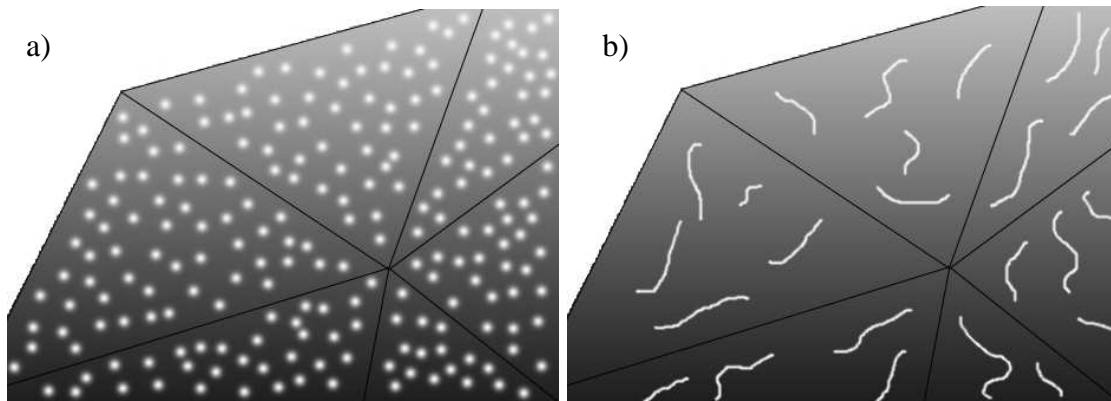


Fig. 1. Abrasive grain microstructure diagrams (magnification ca 10000x)

- a) Grains of submicrocrystalline sintered corundum
- b) Grains of nanocrystalline sintered corundum

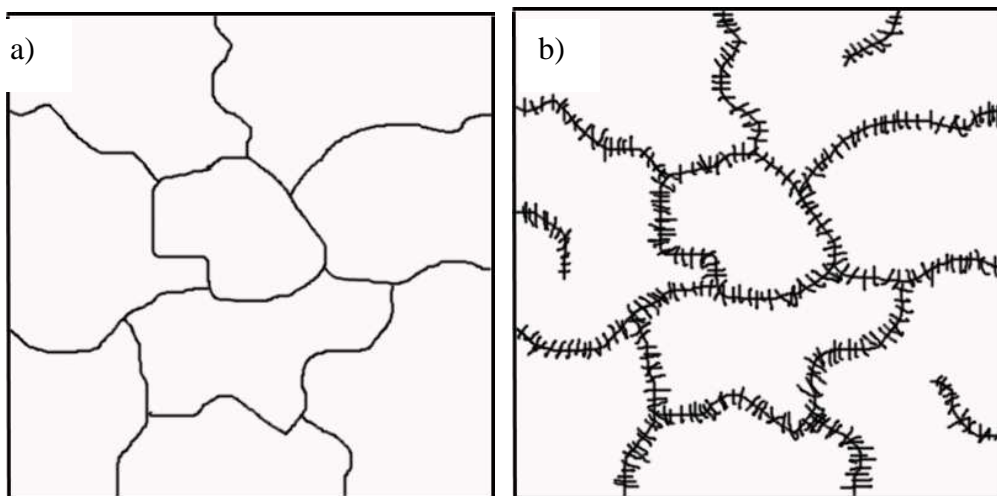


Fig. 2. Ceramic grinding binder diagrams (magnification ca 10000x)

- a) Classical, b) Glasscrystalline

Consequently, new and improved binders are required to maintain grains on the active grinding wheel surface (AGWS). Such conditions are met by recrystallized glass binders of the types 604W and 904W developed in the research laboratories of Rappold Wintherthur, originating from cooling in low temperatures, that display nearly 20% higher durability than the classical silt-feldspar-kaolin ceramic binders. Such binders were used for the production of NanoWin™ grinding wheels belonging to the most recent generation of hard abrasives. According to the manufacturer's data, NanoWin™ grinding wheels are characterized by repeatable and constant hardness, 10% lower binder proportion, 10% higher pore volume, 30% lower probability of grinding burn occurrence on the machined surfaces and the smoothing grinding-cutting effect produced by the crystalline chains contained in the binder [3,4].

2. GRINDING WHEEL'S CUTTING CAPACITY AND COMBINED INDICATORS FOR DETERMINATION OF THAT CAPACITY

The grinding wheel cutting capacity is defined as its capability to separate proper quantity of material in a unit of time, in specific grinding conditions, with the observation of the required surface quality of the machined surface and with the lowest possible expenditures. The definition indicates that the grinding wheel's cutting capacity is a complex conception that entails geometric, physical, technological and economic criteria depending on needs. [1] As to geometric criteria, we usually use such indicators as radial or thickness grinding-wheel wear, grinding-wheel weight or volume reduction and ground-off material's weight or volume. However, as to the technological indicators, the ones most often used are: the machined surface roughness parameters Ra, Rz and Rm, plateau area Rmr(c), as well as the machined product's dimensional and shape accuracy. The dominating physical indicators are such as the radial or circumferential components of the grinding force, active grinding force and grinding area temperature. The economic indicators may be chosen in a number of ways, either as economic-technological ones (e.g. grinding wheel's durability), or purely economic ones (e.g. unit grinding cost). Table 1 shows selected combined indicators for the evaluation of the grinding wheel's cutting capacity in a chronological sequence.[1]

Table 1. Combined grinding wheel cutting capacity indicators

Developers' Names and Years of Completion								
G. Schlesingr 1927	Norton 1943	McKee- Moore I 1948	McKee- Moore II 1950	W. Wolfram Takadzawa Jokojama 1952	W. Majkus 1954	Lurie I 1956	Lurie II 1965	Lurie Nizankowski 1984
$\frac{V_{mt}}{V_{st}}$	$\frac{V_{mt}^2}{V_{st}}$	$\frac{V_{mt}}{V_{st} \cdot P \cdot Ra}$	$\frac{Q_m}{F_v}$	$\frac{V_{mt}}{V_{st}} \cdot F_v$	$\frac{t_m}{F_p}$	$\frac{Q_m}{F_p}$	$\frac{Q_m}{F_v} \cdot T$	$\frac{Q_m}{P}$

Where:

V_{mt} – ground-off material volume in time t ,

V_{st} – grinding wheel volume loss in time t ,

P – active grinding wheel drive-motor power,

R_a – average arithmetic deviation of the roughness profile of the machined surface from the average line,

F_v – circumferential component of the grinding force,

t_m – machine grinding time,

F_p – radial component of the grinding force,

Q_m – grinding capacity,

Θ – temperature in the grinding zone.

The first McKee-Moor indicator was adopted for the purpose of comparative studies of the cutting capacities of the previously specified grinding wheels.

3. TEST METHODOLOGY AND TECHNIQUES

The comparative experimental tests on the cutting capacity of the noble alundum grinding wheels with classical ceramic binder, grinding wheels made of the mix of submicrocrystalline sintered corundum and noble alundum on low-melting glasscrystalline binder, and grinding wheels made of the mix of nanocrystalline sintered corundum and noble alundum on recrystallized glass binder were conducted in accordance with a single-factor, static, determined and complete PS/DK test plan [2]. In the adopted test schedule, the grinding time was the input variable, while the active grinding-wheel drive-motor power and the R_a machined surface roughness parameter were the output variables. The fixed values included the grinder type (STD) used for grinding, the parameters of the grinding wheels applied (1A 250x32x76 38A 60G12V, 1A 250x32x76 5 SG60G12V5, and 1A 250x32x76 55N60F15VPH), the grinding conditions ($V_c=35$ m/s, $V_f=18$ m/min, $f_p=16$ mm/2x feed, stroke $a_n=0,015$ mm), grinding method (rough, circumferential surface grinding, using a grinder with a rectangular table), CLL cooling and lubricating liquid (5% oil-in-water emulsion), machined material (hardened steel with the hardness of 64 ± 2 HRC), grinding cycle (three stages) and the initial honing method and parameters (single-grain, diamond, collarless honing tool M3010, 0.8 kr, honing depth: $a_\alpha=0.01$, number of passes: $i_\alpha=2$, coverage index: $k=2$, honing feed $f_o=0.02$ mm/rot.). The dispersion of physical and chemical material properties of the grinding-wheels, machined objects and CCS, as well as inaccuracies in the performance of the accepted machining parameters, honing and input value measurements were accepted as interfering values. Output value measurements were taken every 10 minutes. In no test plan system, replication of experiments was conducted because of a limited quantities of grinding wheels. The grinding-wheel cutting-capacity tests were interrupted when the machined surface showed the initial bloom during grinding, indicating a possibility of occurrence of the so-called grinding burns. In such cases, the preceding experiment system specified in the test plan was considered to be the last one. The machined object's volume loss was determined by measuring the loss of the sample's height, using a Zeiss cogged clock sensor, with the elementary graduation of 0.001 mm,

followed by recalculation of the volume. The grinding wheel's volume loss was determined by the Salje method (base stroke technique), grinding wheel's base motor's active power was determined by application of two wattmeters connected in the Aron's system, while the value of parameter Ra was determined with the use of a Hommel Werke profile meter. Each of the output volumes was measured three times in each experiment plan system.

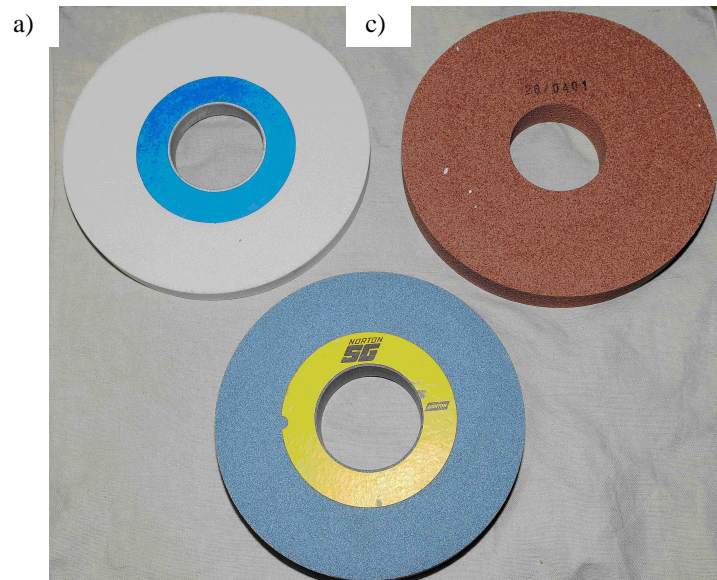


Fig. 3. Picture of the (b) grinding wheels applied in the comparative experimental tests:
a) 99A; b) 99A+SG; c) 99+N

4. TEST RESULTS AND ANALYSIS

The results of the ground-off material volume changes, depending on the kind of abrasant and grinding time, are presented in Table 2.

Table 2. Changes in the ground-off material volume V_{mt} [mm³], depending on the kind of abrasant and grinding time t [mins.]

	10	20	30	40	50	60	70	80	ToGBO
99A	899 912 965	1692 1800 1746							23
SG+99A	970 1014 1006	1900 1853 1866	2812 2901 2942	4002 3983 3968	4830 4920 4949	5892 5931 5814			67
N+99A	1035 1052 1069	1989 2013 2048	2990 2936 2989	4103 4075 4112	5122 5143 5164	6066 6102 6151	7060 7090 7127	8000 8072 8143	89

The results of the grinding wheel volume changes, depending on the kind of abrasant and grinding time, are presented in Table 3.

Table 3. Changes in the grinding wheel volume V_{st} [mm³], depending on the kind of abrasant and grinding time t [mins.]

	10	20	30	40	50	60	70	80	ToGBO
99A	277	353							23
	250	370							
	238	349							
SG+99A	252	332	413	532	609	720			67
	233	340	452	548	642	735			
	246	328	469	577	656	728			
N+99A	239	322	422	508	600	689	769	893	89
	224	370	441	519	621	695	784	880	
	211	351	437	530	632	715	798	869	

In Tables 4 and 5, the changes in the active grinding-wheel drive-motor power and the values of parameter Ra of the machined surface roughness are presented, respectively.

Table 4. Changes in the active grinding-wheel drive-motor power P [kW], depending on the kind of abrasant and grinding time t [mins.]

	10	20	30	40	50	60	70	80	ToGBO
99A	1.81	2.09							23
	1.66	1.93							
	1.72	1.99							
SG+99A	1.74	1.96	2.01	2.32	2.39	2.36			67
	1.67	1.79	1.92	2.27	2.41	2.35			
	1.61	1.87	1.89	2.18	2.34	2.28			
N+99A	1.64	1.73	1.88	2.02	2.24	2.32	2.48	2.33	89
	1.58	1.67	1.79	2.10	2.18	2.23	2.39	2.27	
	1.51	1.69	1.90	2.03	2.11	2.19	2.44	2.19	

Table 5. Changes in the parameter Ra [μ m] of the machined surface roughness values, depending on the kind of abrasant and grinding time t [mins.]

	10	20	30	40	50	60	70	80	ToGBO
99A	0.89	0.74							23
	0.93	0.69							
	0.86	0.65							
SG+99A	0.78	0.71	0.63	0.61	0.57	0.63			67
	0.74	0.68	0.63	0.59	0.54	0.59			
	0.71	0.64	0.60	0.63	0.52	0.61			
N+99A	0.69	0.66	0.62	0.59	0.50	0.46	0.39	0.48	89
	0.68	0.63	0.58	0.52	0.48	0.41	0.37	0.45	
	0.65	0.61	0.55	0.54	0.42	0.40	0.36	0.49	

Our tests allowed us to calculate the first McKee-Moor indicator of the cutting capacities of the tested grinding wheels in particular experiment plan systems:

$$W_{zs} = \frac{V_{mt}}{V_{st} \cdot P \cdot Ra} \Big|_{ToGBO} \quad \frac{1}{kW \cdot \mu m} \quad (1)$$

Where:

ToGBO - time of grinding burn occurrence,

W_{zs} – grinding wheel cutting capacity indicator of McKee-Moor (I) as presented in Table 6. and illustrated in Fig. 4.

Table 6. Changes in the cutting capacity indicator values, depending on the kind of abrasant and grinding time

	10	20	30	40	50	60	70	80	ToGBO
99A	2.01 2.36 2.74	3.09 3.65 3.86							23
SG+99A	2.83 3.67 3.57	4.11 4.47 4.75	5.37 5.31 5.53	5.31 5.42 5.01	5.82 5.89 6.20	5.50 5.82 5.74			67
N+99A	3.82 4.37 5.16	5.41 5.17 5.66	6.08 6.41 6.54	6.78 7.19 7.08	7.62 7.91 9.22	8.25 9.60 9.82	9.49 10.22 10.17	8.01 8.98 8.73	89

The obtained results of the cutting capacity indicator value calculation results were subjected to approximations, using the functions in the form of the second-degree polynomial, while the approximation errors were determined by calculation of the values of the so-called determination coefficients.

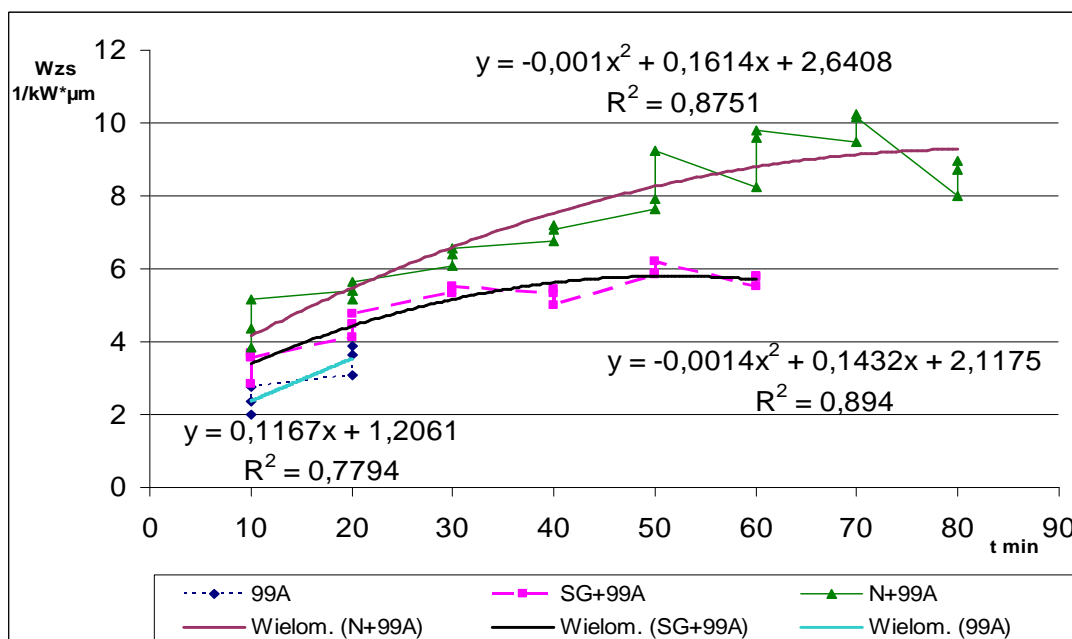


Fig. 4. Approximation of the cutting capacity indicator value calculation results

5. CONCLUSIONS

As a result of the completed comparative experimental tests on the cutting capacities of the three different types of grinding wheels, we concluded as follows:

- The first McKee-Moor cutting-capacity indicator applied in our tests was correctly adopted and it reproduced well the changes in the cutting capacities of particular types of grinding wheels.
- In the process of grinding of the hardened-steel surfaces, the cutting capacities of the grinding wheels containing only abrasives 99A, 50%SG+50%99A and 55%N+99A indicated considerable differences, while the NanoWin™ grinding wheels were characterized by the highest cutting capacity in the whole grinding period.
- The durability of the particular types of the grinding wheels also differed essentially, and the approximate durability relationships were the following: 1 (99A) : 3 (SG+99A) : 5 (N+99A).

REFERENCES

- [1] NIŻANKOWSKI CZ., OTKO T., Badania porównawcze zdolności skrawnych taśm ściernych typów BTX22-5 i BTX22-6 przy obróbce stopu tytanu Ti-6Al-4V., Monografia, Wybrane problemy obróbki ścierniej, Wydawnictwo Politechniki Krakowskiej, Bochnia 2008, 251-260.
- [2] POLAŃSKI Z., Planowanie doświadczeń w technice. PWN, Warszawa 1984, 73-97.
- [3] Rappold Winterthur, NanoWin™ Grinding Whells. Catalogue of Company. Villach 2008.
- [4] <http://www.rappold-winterthur.com>